Imai, K. (1978) in *Allosteric effects in haemoglobin*, Cambridge University Press, Cambridge, U.K.
Imai, K., Yonetani, T., & Ikeda-Saito, M. (1977) *J. Biol. Chem. 109*, 83-97.
Ip, S. H. C., Johnson, M. L., & Ackers, G. K. (1976) *Biochemistry 15*, 654-660.
Johnson, M. L., Halvorson, H. R., & Ackers, G. K. (1976) *Biochemistry 15*, 5363-5371.
Mills, F. C., & Ackers, G. K. (1979a) *J. Biol. Chem. 254* (8), 2881-2887.
Mills, F. C., & Ackers, G. K. (1979b) *Proc. Natl. Acad. Sci. U.S.A. 76* (1), 273-277.
Mills, F. C., Johnson, M. L., & Ackers, G. K. (1976) *Biochemistry 15*, 5350-5362.
Nagel, R. L., & Gibson, Q. H. (1971) *Biochemistry 10*, 69.
Pettigrew, D. W., Romeo, P. H., Tsapis, A., Thillet, J., Smith, M. L., Turner, B. W., & Ackers, G. K. (1982) *Proc. Natl. Acad. Sci. U.S.A. 79*, 1849-1853.
Press, W. H., Flannery, B. P., Teukolsky, S. A., & Vetterling, W. T. (1986) in *Numerical Recipes: The Art of Scientific Computing*, p 468, Cambridge University Press, Cambridge.
Speros, P. C. (1990) Ph.D. Dissertation, The Johns Hopkins University.
Speros, P. C., LiCata, V. J., Yonetani, T., & Ackers, G. K. (1991) *Biochemistry* (preceding paper in this issue).
Turner, B. W. (1984) Ph.D. Dissertation, The Johns Hopkins University.
Turner, B. W., Pettigrew, D. W., & Ackers, G. K. (1981) *Methods Enzymol. 76*, 596-628.
Turner, G. J. (1989) Ph.D. Dissertation, The Johns Hopkins University.
Wyman, J., & Gill, S. J. (1990) in *Binding and Linkage: Functional Chemistry of Biological Macromolecules*, University Science Books, Mill Valley, CA.

A Fluorescence Lifetime Study of Virginiamycin S Using Multifrequency Phase Fluorometry†

Koen Clays,‡ Mario Di Giambattista,§ Andre Persoons,‡ and Yves Engelborghs*,‡

Laboratory of Chemical and Biological Dynamics, University of Leuven, Celestijnenlaan 200 D, B-3001 Leuven, Belgium, and Microbiology and Genetics Unit, Institute of Cellular Pathology, University of Louvain Medical School, B-1200 Brussels, Belgium

Received November 26, 1990; Revised Manuscript Received March 7, 1991

ABSTRACT: Using multifrequency phase fluorometry, fluorescence lifetimes have been assigned to the different protolytic forms of the antibiotic virginiamycin S. These lifetimes are 0.476 ± 0.005 ns for the uncharged form, 1.28 ± 0.2 and 7.4 ± 0.2 ns for the zwitterionic form, 1.19 ± 0.01 ns for the negatively charged form, and 1.9 ± 0.1 ns for the double negatively charged form. The assignments are based on lifetime measurements as a function of pH, volume percent ethanol, and excitation wavelength. Excited-state proton transfer is taken into account. It is complete at pH values lower than 1, and no fluorescence of the fully protonated charged form is observed. At pH 8, an excited-state pK^* increase is calculated, but proton association is too slow to cause excited-state proton transfer. The addition of divalent cations, at pH 9.4, increases the lifetime of the negatively charged form to a value dependent upon the specific nature of the cation (7.58 ± 0.06 ns for Mg^{2+}, 6.54 ± 0.02 ns for Ca^{2+}, and 3.74 ± 0.05 ns for Ba^{2+}). Monovalent cations do not influence the lifetimes, indicating that their binding to the macrocycle does not influence the fluorescent moiety. The model compound 3-hydroxypicolinamide shows an analogous behavior, but the retrieved lifetime can differ significantly.

Virginiamycin S (VS)[1] is a hexapeptide with a fluorescent side group (the 3-hydroxypicolinyl group) attached to it through an amide bond. It is an antibiotic because it blocks protein synthesis at bacterial ribosomes (Cocito, 1979). Due to a strong enhancement of the fluorescence of VS upon binding to ribosomes, its binding kinetics could be studied extensively by fluorescence stopped-flow techniques (Moureau et al., 1983; Di Giambattista et al., 1987). Its dissociation rate constant was obtained by displacement studies with erythromycin. Several other antibiotics show partial or complete overlap of their binding site with that of VS, such that their binding could also be studied, using displacement or competition kinetics. In this way, three partially overlapping binding sites could be discerned (Di Giambattista et al., 1987).

VS is only weakly fluorescent in aqueous solutions, but the fluorescence increases strongly in the presence of Mg^{2+} ions. A further intensity increase is observed upon binding to the ribosomes. Responsible for this fluorescence is the 3-hydroxypicolinyl moiety. Quenching studies have shown that this group is buried in the ribosome complex and partially shielded from solvent access (Di Giambattista et al., 1984).

In this paper, a fluorescence lifetime study is described, using multifrequency phase fluorometry. The hydroxypicolinyl group appears in several protolytic forms, and the lifetimes were therefore determined as a function of pH, of the presence of Mg^{2+} ions and ethanol. A comparison between VS and 3-

† K.C. is a research associate and Y.E. is research director of the Belgian National Fund for Scientific Research. Financial support was obtained from the Research Fund of the University of Leuven and from the Belgian National Fund for Scientific Research.

* Correspondence should be addressed to this author.
‡ University of Leuven.
§ University of Louvain Medical School.

[1] Abbreviations: VS, virginiamycin S; 3-HPA, 3-hydroxypicolinamide; SAS, species-associated spectrum.

0006-2960/91/0430-7271$02.50/0

hydroxypicolinamide is made.

Materials and Methods

VS was prepared by RIT (Belgium). Because of the low solubility of VS in water and based on the experience gained in previous studies (Di Giambattista et al., 1984), ethanol p.a. was chosen as the solvent for the stock solution of VS. The solutions used for the experiments at increasing pH values are HCl/KCl, acetate buffer, phosphate buffer, ammonia/HCl, bicarbonate/NaOH, and KCl/NaOH mixtures. The ionic strength was always 0.1 M. As a bacteriostatic, 0.5 mM NaN_3 was added. Final stock solutions contained 25% ethanol, and VS concentration was 25 μM. Solutions with 50% ethanol were prepared from buffers already containing 25% ethanol. Solutions with different concentrations of mono- and bivalent cations were prepared by adding the chlorides KCl, NH_4Cl, $MgCl_2$, $CaCl_2$, and $BaCl_2$ to the buffer with pH 9.4. At this pH, the protolytic form capable of ion binding is predominant. At lower pH, a precipitate was formed immediately.

The VS model compound 3-hydroxypicolinamide (3-HPA) was obtained from Janssen Chimica (Belgium). Comparable solutions were prepared, i.e., with the same buffer and cation content. In this way, a direct comparison could be made between VS and the model compound.

Absorption measurements were performed on a double-beam spectrophotometer (KONTRON UVIKON 860). The corresponding buffer solution without VS was used as the blank.

Steady-state excitation and emission spectra were recorded on an automated spectrofluorometer (SPEX) with a single-grating excitation and a double-grating emission monochromator. Spectra were taken with 2-mm slit width. Wavelength resolution was accordingly 7.2 and 3.6 nm for excitation and emission spectra, respectively. Emission spectra were not corrected for the wavelength dependence of the emission monochromator and the photomultiplier sensitivity. Fluorescence was detected with an analyzing polarizer at 54° in the emission pathway, to eliminate the influence of the wavelength-dependent fluorescence depolarization and Brownian motion on the detected intensity. The cuvette holder was thermostated at 25 °C.

Fluorescence lifetime measurements were performed on a laboratory-built multifrequency phase fluorometer, comparable to the one described by Lakowicz, except for the use of the microchannel plate detector in the latter (Lakowicz et al., 1986). The instrument consists of a cavity-dumped mode-locked dye laser for excitation. A monochromator (Applied Photophysics) is used in emission, and a high-gain photomultiplier (Philips, XP2233B) is used for detection. A detailed description of the instrument has been given (Clays et al., 1989). For measurements of the fluorescence decay parameters of VS and 3-HPA, two different dyes were used in the dye laser, i.e., Rhodamine 6G and DCM [4-(dicyanomethylene)-2-methyl-6-[*p*-(dimethylamino)styryl]-4*H*-pyran]. After frequency doubling, this enabled us to excite at the wavelengths 296 and 330 nm. The cavity-dumped mode-locked dye laser system produces pulses with approximately 20-ps pulse width and with a repetition frequency of 400 kHz. According to the Fourier theorem, such a periodic excitation corresponds to a sum of all the harmonics of 400 kHz up to several tens of gigahertz. The phase measurements were performed at a much lower frequency, obtained by the cross-correlation technique. Two phase-locked frequency synthesizers were used to drive the mode-locker crystal and the gain of the photomultiplier with a frequency difference of 700 Hz. This allowed the phase to be measured accurately at the frequency of the lower cross-correlation product, i.e., 700 Hz. Phase measurements were performed at 50 harmonics of the repetition frequency. Since a phase difference can be measured much more accurately than a modulation, it was preferred to make more phase measurements, at different frequencies. Phase shifts and standard deviations at this number of frequencies were analyzed for the fluorescence decay parameters by the nonlinear least-squares Marquardt algorithm on a MicroVAX 2000 minicomputer. Statistical parameters, such as the reduced χ^2, the standard normally distributed χ^2, the quality of fit, the mean and standard deviation of the weighted residuals, and graphical tests, such as a residual plot and a plot of the autocorrelation function of the weighted residuals, were used to decide whether the fluorescence decay is single, double, or triple exponential. Especially the autocorrelation function of the weighted residuals proved useful in model discrimination. Analyzing phase shifts and their standard deviations at these 50 frequencies, but also at different emission or excitation wavelengths, has been performed by global analysis. The fluorescence lifetimes were floating parameters in the fitting procedure, but constrained to be the same over the whole spectrum, while the fractional contributions remained independent at every wavelength. Global analysis of the experimental data reduced the uncertainty in the recovered decay parameters. When the fluorescence proved to be heterogeneous, decay-associated spectra could be reconstructed very accurately from the fractional contributions. In this way, a steady-state fluorescence spectrum can be resolved in different contributions. These spectra are species-associated whenever a lifetime can be attributed to a single species.

Results

Influence of pH. (A) Absorbance and Fluorescence Spectra. pH titration studies of VS have been performed (Grell et al., 1979). These revealed the presence of different absorption spectra which could be linked to the different protolytic forms. A scheme of the protolytic reactions for VS, together with the definitions of the equilibrium constants for the reactions and the symbols for the species, is shown in Figure 1. The concentration of the different species can be calculated from these equilibrium constants as a function of pH and is shown in Figure 2. At very low pH values (pH <2), an absorption band at 303 nm is observed which can be attributed to the fully protonated (P^+) form. Increasing the pH to values between 2 and 4 induces a strong red shift to 355 nm. This 355-nm component is attributed to the zwitterionic form ($P^\pm$). Further increasing the pH to about 9 (respectively 12) causes a blue shift to 339 nm (respectively 330 nm). These absorption bands are attributed to the P^- and P^{2-} forms, respectively.

Excitation spectra of VS at different pHs, recorded with the emission wavelength at 420 nm, show the same features. However, the peaks between 330 and 350 nm contribute more to the fluorescence intensity than the 303-nm band.

Emission spectra, taken with 330-nm excitation wavelength, show a broad peak throughout the whole pH range. The intensity varies with the pH, the highest values being detected at the highest pH. A small shoulder is observed at the short-wavelength side of the emission maximum only for the solutions with high pH (pH 7.6 and higher). The emission spectra for VS at different pH values are shown in Figure 3.

(B) Lifetime Analysis. Fluorescence lifetime analysis clearly revealed the presence of multiple lifetimes at different pH values. The results of a series of phase measurements at pH 4.2 are shown in Figure 4. The curve fitting and the statistical parameters show that the phase data are best described by a

Table I: Fluorescence Lifetimes and Fractional Contributions of VS at Different pHs (Excitation 330 nm, Emission 420 nm, Single-Wavelength Analysis)

pH	τ_1 (ns)	f_1	τ_2 (ns)	f_2	τ_3 (ns)	f_3
1.2	0.45 (0.03)[a]	0.84 (0.09)	1.25 (0.3)	0.16 (0.09)		
2.6[b]	0.476 (0.005)	0.84 (0.02)	1.28 (0.2)	0.14 (0.01)	7.4 (0.2)	0.01 (0.01)
4.2	0.48 (0.05)	0.65 (0.11)	1.3 (0.4)	0.21 (0.10)	7.2 (0.5)	0.14 (0.10)
7.4	1.1 (0.1)	0.75 (0.05)	1.7 (0.4)	0.25 (0.05)		
9.4	1.1 (0.1)	0.85 (0.04)	1.7 (0.7)	0.15 (0.04)		
11.0	1.2 (0.1)	0.60 (0.05)	1.9 (0.2)	0.40 (0.05)		
12.6			1.7 (0.1)	0.91 (0.05)	2.7 (1.8)	0.09 (0.05)

[a] Values in parentheses are estimated uncertainties. [b] Results of global analysis; single-wavelength analysis reveals the double exponential with two mean lifetimes.

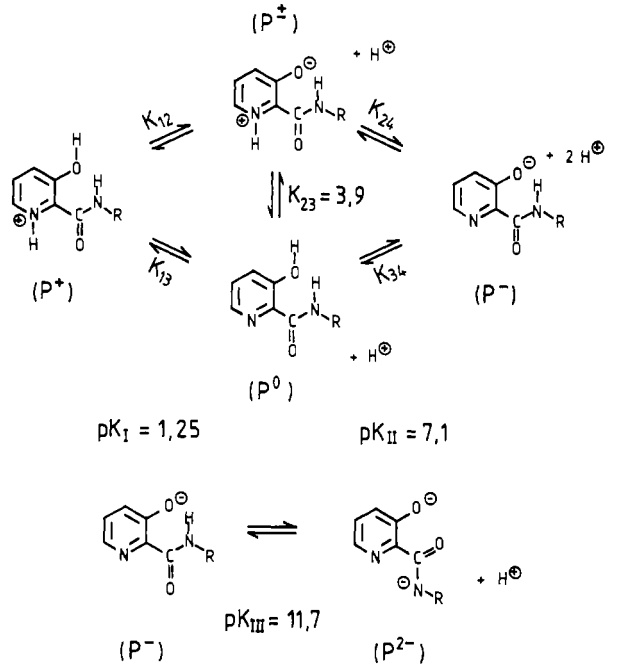

FIGURE 1: Scheme of the protolytic reactions of VS, with the associated equilibrium constants. $K_I = K_{13} + K_{12}$ and $K_{II} = (K_{24} + K_{34})/K_{34}K_{24}$ are the global dissociation constants for the first and the second deprotonation.

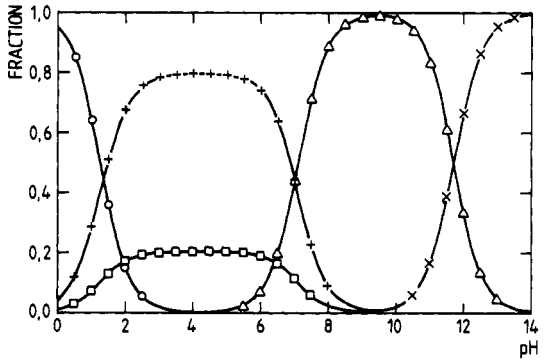

FIGURE 2: Plot of the relative concentrations of the different protolytic forms of VS as a function of pH, calculated on the basis of the equilibrium constants given Figure 1. (○) P^+, (+) $P^{\pm}$, (□) P^0, (△) P^-, and (×) P^{2-}.

sum of three exponentials. The results of similar lifetime measurements of VS as a function of pH are compiled in Table I. Lifetime measurements were performed across the whole emission spectrum of VS, from 390 to 480 nm, with an interval of 10 nm. These data were analyzed by the global analysis method. The individual spectra, associated with each lifetime, were reconstructed. Figure 5 shows these decay-associated spectra (DAS) for VS at pH 11.0. The two components with a different lifetime also have a different emission spectrum. The shorter lived component (1.19 ± 0.01 ns) shows a blue-shifted emission with a maximum at 400 nm, while the longer lived component (1.9 ± 0.2 ns) has an emission maximum at 420 nm. The blue-shifted contribution of this protolytic form is also observed as a shoulder in the steady-state emission spectrum at high pH (pH 7.6 and higher, Figure 3A–D). Phase measurements were also performed with excitation at 296 nm. At pH 12.6, the fluorescence decay of VS was singly exponential as judged by the graphical tests and numerical fit parameters. All the phase data obtained as a function of emission and excitation wavelength and pH were analyzed simultaneously by the global analysis method. This enables the retrieval of a very small contribution of a particular pro-

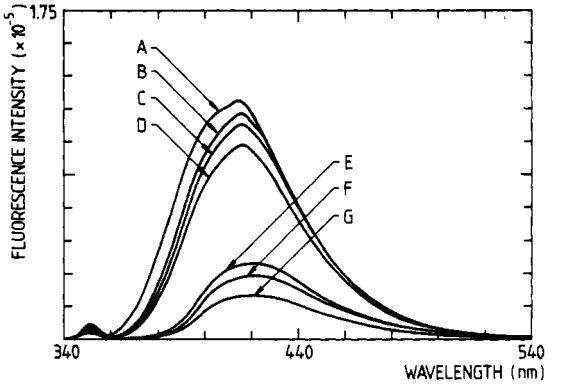

FIGURE 3: Uncorrected emission spectra of VS at different pH values. Excitation at 330 nm. (A) pH 12.6; (B) pH 11.0; (C) pH 9.6; (D) pH 7.6; (E) pH 4.1; (F) pH 2.6; (G) pH 1.1.

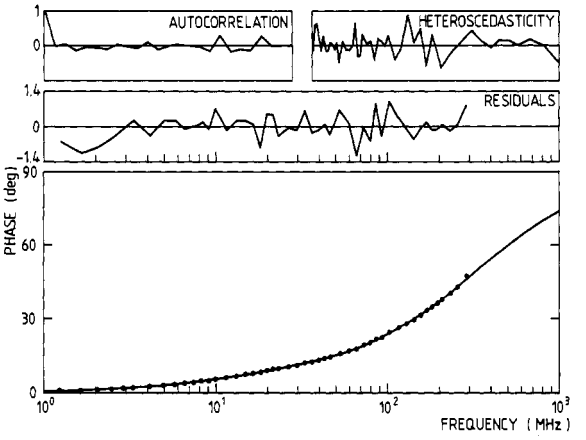

FIGURE 4: Phase measurement of VS at pH 4.2 and graphical tests for a fit to a triple-exponential fluorescence decay. (Main figure) The phase angle (in degrees) is plotted versus the frequency (logarithmic scale): (●) measured points and their errors; (—) fitted line. Weighted residuals are plotted as a function of frequency (residuals). The autocorrelation function of the weighted residuals is given as well as the heteroscedasticity plot, i.e., the plot of the weighted residuals as a function of the calculated phase angle; reduced $\chi^2 = 0.34$; standard normally distributed $\chi^2 = -3.8$; quality of fit = 1.00; mean of weighted residuals = 0.04; standard deviation of weighted residuals = 0.83; percentage of weighted residuals in the interval −2,+2 = 100.

Table II: Fluorescence Lifetimes and Fractional Contributions of Virginiamycin S in pH 4.2 Buffer with Different Ethanol Content (Excitation 330 nm, Emission 420 nm, Single-Wavelength Analysis)

vol % ethanol	τ_1 (ns)	f_1	τ_2 (ns)	f_2	τ_3 (ns)	f_3
25	0.49 (0.05)[a]	0.70 (0.05)	1.3 (0.3)	0.20 (0.05)	7.2 (0.5)	0.10 (0.05)
50	0.51 (0.07)	0.92 (0.04)	1.4 (0.7)	0.07 (0.04)	6.3 (1.0)	0.01 (0.04)

[a] Values in parentheses are estimated uncertainties.

Table III: Fluorescence Lifetimes and Fractional Contributions of Virginiamycin S at pH 9.4 with Different Concentrations of Cations (Excitation 330 nm, Emission 420 nm, Single-Wavelength Analysis)

cation	[cation] (mM)	τ_1 (ns)	f_1	τ_2 (ns)	f_2
none		1.1 (0.1)[a]	0.85 (0.04)	1.7 (0.7)	0.15 (0.04)
K^+	20	1.21 (0.07)	0.92 (0.03)	2.2 (0.8)	0.08 (0.03)
	100	1.0 (0.3)	0.92 (0.03)	1.5 (0.4)	0.08 (0.03)
NH_4^+	20	1.23 (0.01)	0.95 (0.02)	2.2 (0.4)	0.03 (0.02)
	100	1.1 (0.1)	0.90 (0.03)	2.0 (0.3)	0.10 (0.03)
Mg^{2+}	5	1.19 (0.02)	0.20 (0.02)	7.67 (0.03)	0.80 (0.02)
	20	1.14 (0.09)	0.08 (0.01)	7.58 (0.06)	0.92 (0.01)
Ca^{2+}	20	1.21 (0.02)	0.15 (0.02)	6.55 (0.02)	0.85 (0.02)
	100	1.17 (0.01)	0.04 (0.01)	6.54 (0.02)	0.96 (0.01)
Ba^{2+}	20	1.18 (0.05)	0.55 (0.02)	3.3 (0.2)	0.45 (0.02)
	100	1.30 (0.05)	0.25 (0.03)	3.74 (0.05)	0.75 (0.03)

[a] Values in parentheses are estimated uncertainties.

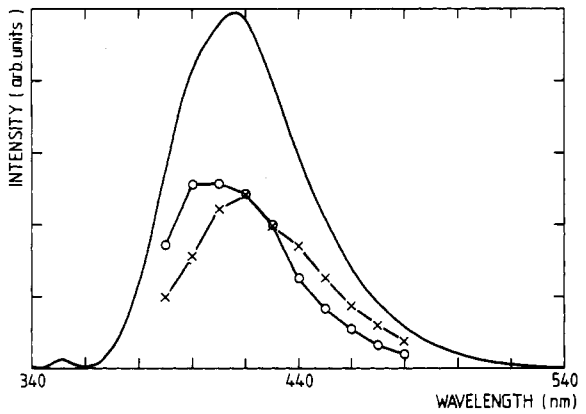

FIGURE 5: Decay-associated spectra recovered from global analysis of the phase data obtained at pH 11.0. (O) DAS of the shorter lived component (1.19 ns); (×) DAS of the longer lived component (1.9 ns); (upper solid line) steady-state emission spectrum of VS at pH 11.0.

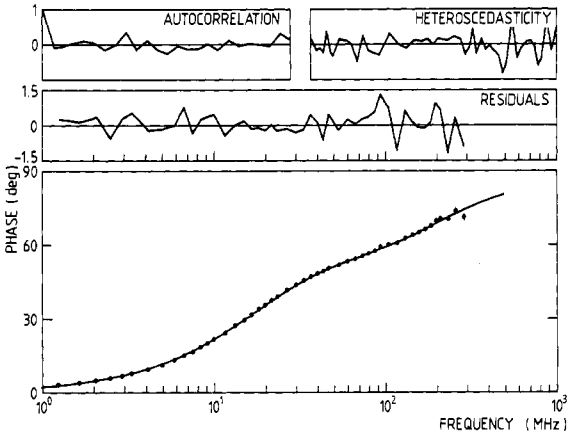

FIGURE 6: Phase measurement of VS at pH 9.4 with 5 mM Mg^{2+} and graphical tests incorporated in the data reduction for a fit to a double-exponential fluorescence decay: reduced $\chi^2 = 0.34$; standard normally distributed $\chi^2 = -3.9$; quality of fit = 1.18; mean of weighted residuals = 0.08; standard deviation of weighted residuals = 0.83; percentage of weighted residuals in the interval −2,+2 = 100.

tolytic form at an intermediate pH (e.g., at pH 2.6).

Effect of Ethanol. Around pH 4, the equilibrium between the zwitterionic and the neutral form can be displaced by variation of the total amount of ethanol in the solution. Two solutions were prepared, with ethanol contents of 25 and 50%. The higher ethanol content resulted in an increase of the absorbance of the 303-nm band and a decrease of the absorbance of the 355-nm band. Excitation spectra (not shown) confirm this observation. The emission intensity of the solution with 50% ethanol was decreased. The same lifetimes are measured in both solutions, but the fractional contributions differ. Results of the lifetime measurements on both solutions are compiled in Table II. Additional information useful for the association of absorption bands to different protolytic forms with a specific lifetime is gained by excitation at 296 nm instead of at 330 nm.

Influence of the Addition of Cations. The influence of cations was also investigated, because it is known that VS is able to bind to different cations at different sites. These measurements were performed on buffer solutions with pH 9.4, because the protolytic form capable of ion binding is predominant at this pH. Addition of monovalent cations showed only a very small influence on absorption, excitation, and emission spectra. The fluorescence decay was biexponential, as was the case for VS without cations at pH 9.4. The fluorescence lifetimes were not dependent on the nature of the monovalent cation and remained the same when different amounts of monovalent cations were added. The influence of addition of divalent cations was more pronounced. Absorption spectra were slightly red-shifted upon addition of divalent cations. The emission spectra showed a large increase in intensity. Measurements on the phase fluorometer revealed a biexponential fluorescence decay for each divalent cation, with the lifetime of the longer lived component dependent upon the nature of the cation. Fractional contributions were a function of the concentration and the nature of the cation. Figure 6 shows phase data together with graphical and numerical tests for a measurement on the influence of 5 mM Mg^{2+}; Table III summarizes the results of these measurements.

Results with 3-HPA, a Model Compound for VS. Since 3-HPA is the fluorescent moiety of VS, a number of observations were checked for this compound. An estimation of the influence of the peptide–lactone ring could be made, because direct comparison between VS and 3-HPA is possible. Absorption spectra as a function of pH show the same bands as for VS. Differences in band intensities at the various pH values are explained by the differences in pK values for 3-HPA with respect to VS. These observations are confirmed in

excitation spectra. The emission spectra are influenced by pH in the same way as for VS: lower intensity at low pH, higher at higher pH. The fluorescence decay of 3-HPA at pH 12.6 with excitation at 296 nm is very well described by a single exponential with a decay time of 1.048 ± 0.005 ns. Addition of ethanol has the same influence on 3-HPA as on VS: the 303-nm band increases in intensity, while the 355-nm one decreases. The same changes are observed in excitation spectra. The influence on the emission is merely a decrease in intensity, as anticipated. The influence of added cations is also analogous.

Discussion

Absorption Spectra. The pH dependence of the absorption properties of VS is readily explained in terms of the different protolytic forms of the antibiotic, each with different charge densities at the electron donor or acceptor groups (Grell et al., 1979). A scheme of the protolytic reactions for VS, together with the equilibrium constants for the reactions, is shown in Figure 1. The relative contribution of the different protolytic forms as a function of pH, calculated on the basis of these equilibrium constants, is shown in Figure 2. At very low pH values, the fully protonated form is obtained, characterized by a band at 303 nm. A big red shift to 355 nm appears upon the first ionization. At pH 4.2, two different protolytic forms are present: the zwitterionic form $P^{\pm}$ and the neutral form P^0. The absorption spectrum also shows two bands, with a spectral shift of roughly 50 nm. The shorter wavelength band can be attributed to the neutral form P^0. The longer wavelength band is associated with the zwitterionic form $P^{\pm}$. Evidence for this attribution is found in the fact that in solutions containing more ethanol, the lower wavelength absorption band is increased. The neutral P^0 form is more readily stabilized in alcoholic solutions than is the zwitterionic form $P^{\pm}$. Increasing the pH further to 9.4 removes the second proton and induces a blue shift to 339 nm. A further blue shift to 330 nm is obtained when the amide proton is removed.

Fluorescence Spectra. The correspondence of the excitation spectra with the absorption spectra proves that all absorbing species contribute to the measured fluorescence. Surprisingly, therefore, is the fact that emission only shows a single-wavelength maximum. This can, however, be explained on the basis of a strong pK shift in the excited state, as indicated by the shift in absorbance wavelength. On the basis of the Förster cycle and assuming equal vibrational energy relaxation in both protolytic forms, the pK^* for the first ionization can be calculated to be $pK_I^* = -8.9$. The kinetics of the protolytic reactions of hydroxypyridine have been studied extensively (Schuster et al., 1976). Schuster et al. showed that the association of the proton is diffusion-controlled for the ground state. Assuming the same situation for the excited state at pH 1.2, dissociation of the proton from the excited state of the fully protonated form must be extremely rapid, and the reequilibration is established on a subnanosecond time scale. This also explains why only the singly deprotonated form contributes to the emission spectrum and justifies our neglect of emission wavelength in the Förster cycle calculation. Upon increasing the pH from 4.6 to 7.4, a blue shift of 16 nm was observed. Using again Förster cycle calculations, it is found that the pK_{II}^* is now shifted to higher pH values by 2.7 units. This means that after excitation, the protonation equilibrium shifts to the more acidic form. However, at the high pH values used, the rate of H^+ binding can be neglected on the nanosecond time scale, and the system behaves as a heterogeneous mixture of two protolytic forms. This is confirmed by the lifetime studies.

Table IV: Fluorescence Lifetimes and Estimated Uncertainties for the Different Protolytic Forms of VS (Global Analysis)

form[a]	lifetime (ns)	estimated uncertainty (ns)
P^0	0.476	0.005
$P^{\pm}$	1.28	0.2
	7.4	0.2
P^-	1.19	0.01
P^{2-}	1.9	0.2

[a] For the structures of the different protolytic forms, refer to Figure 1.

Fluorescence Lifetimes. The attribution of the different lifetimes is based on the appearance and disappearance of their fractional contributions with changing pH and ethanol concentrations. It should be noted that the fluorescence fractions are not equal to the concentration fractions of the species (as given in Figure 2) since their absorbance coefficients and their quantum yields are not necessarily the same. Taking into account the results of the calculations of excited-state proton transfer, the lifetime of the excited state of the fully protonated form is extremely short and cannot be calculated. To the zwitterionic $P^{\pm}$ species, two fluorescent lifetimes are attributed, 7.4 and 1.3 ns, since these contributions increase when the pH is raised from 2.6 to 4.6 and decrease at higher pH values or when the ethanol concentration is increased (Table IV). The existence of two lifetimes for the same species indicates the existence of two conformers.

To the excited P^0 species, essentially the lifetime of 0.45 ns is given, a contribution that increases with ethanol concentration and disappears at pH values higher than 4.2.

To the excited state of the P^- species, the lifetime of 1.1 ns is assigned, because this contribution appears at pH 7.4, increases when the pH is increased to 9.4, and decreases again at pH 11.

To the excited state of the P^{2-} species, the lifetime of 1.7–1.9 ns is attributed, which increases when the pH is increased from 9.4 to 11 and further to 12.6. The high contribution of 25% of 1.7 at pH 7.4 is probably an error.

The fact that the same lifetimes are consistently found with different excitation wavelengths and even in solutions of different ethanol content is a good indication of ground-state heterogeneity only, without excited-state reactions. All fluorescence phase shift curves are very well fitted to a sum of exponentials, without the need of modifying the fitting function to incorporate excited-state reactions.

Addition of Cations. Monovalent cations added to solutions of VS have no influence on absorption, excitation, and emission spectra, and also not on the fluorescence decay parameters. A cavity formed by the peptide–lactone ring has been suggested as the binding site for these ions. The peptide–lactone ring can adopt a conformation suitable for coordination of alkali ions, similar to the conformation of cyclic peptides and depsipeptides, which are known to exhibit alkali ion specificity (Oberbaumer et al., 1979). Since the fluorescent group is located away from this ring, it is not influenced by the presence of the monovalent cations, buried in the ring. Divalent cations are known to bind to the hydroxypicolinyl residue, and a considerable spectral shift is anticipated. From this, it has been concluded that the protolytic state P^- of VS is coordinated to the alkaline earth ions (Oberbaumer et al., 1979). With the time-resolved measurements, we should be able to test this hypothesis, since we have shown that each protolytic form has one or two characteristic lifetimes. However, the fluorescence decay parameters are also affected by the complexation. The lengthening of the fluorescence lifetimes is attributed to a reduced nonradiative decay rate, caused by the complexation.

It is believed that the complexation of alkaline earth ions occurs by the phenolate oxygen with participation of the amide carboxyl group. In this way, the number of degrees of freedom for nonradiative relaxation is substantially reduced, with the lengthening of the fluorescence lifetimes as a consequence. An analogous long lifetime, but with only a minor contribution, is observed for the P^* form around pH 4, suggesting the presence of the same rotamer at a lower concentration. The difference in lifetime with different metal ions can be rationalized in terms of the heavy-atom effect: the heavier the atom, the larger the spin–orbit coupling and the larger the singlet–triplet intersystem crossing rate. The fractional intensity contributions of the long lifetime reflect the degree of complexation as a function of the concentration and of the nature of the cation. The larger the cation, the lower the complexation constant seems to be. This is an indication that the interaction is predominantly electrostatic in nature, since the effective charge, or the charge density, is lower for the larger cations, causing the reduced interaction.

3-HPA—A Model Compound for VS. The results obtained with the model compound 3-HPA all confirm the previous observations and attributions. The hydroxypicolinyl residue is clearly the absorbing and fluorescent chromophore in the wavelength range mentioned, and it is also the group responsible for the alkaline earth ion complexation and proton-transfer properties of VS. The peptide–lactone ring, however, is responsible for the alkaline ion complexation, but this does not affect the chromophore. The ring also has a pronounced influence on the value of the lifetime of the hydroxypicolinyl group attached to it: At pH 12.6, the lifetime of 3-HPA of 1.048 ns is increased to 1.77 ns for VS. This increase in excited-state lifetime could reflect a lower rate of nonradiative relaxation, due to a decrease of the degrees of freedom imposed by the binding to the decapeptide ring.

Conclusions

The influence of pH and addition of mono- and divalent cations on the fluoresence decay of VS could be rationalized in terms of the different fluorescent lifetimes of the protolytic forms of VS. The lifetime of the negatively charged form is increased by the presence of divalent cations due to a decreased nonradiative relaxation rate. The decapeptide ring of VS also has an influence on the lifetime of its fluorescent moiety. On the basis of the Förster cycle, excited-state proton-transfer reactions could be shown. In acid medium, this leads to the observation of the fluorescence of the neutral form only. In basic medium, an excited-state pK^* increase is calculated, but association of the proton is too slow in comparison with radiative decay.

Acknowledgments

We thank Françoise Marvellie for technical assistance and Luc Parys for the skillful graphical work.

Registry No. VS, 23152-29-6; 3-HPA, 933-90-4; Mg, 7439-95-4; Ca, 7440-70-2; Ba, 7440-39-3; ethanol, 64-17-5.

References

Clays, K., Jannes, J., Engelborghs, Y., & Persoons, A. (1988) *J. Phys. E 22*, 297–305.

Cocito, C. (1979) *Microbiol. Rev. 43*, 145–198.

Di Giambattista, M., Ide, G., Engelborghs, Y., & Cocito, C. (1984) *J. Biol. Chem. 259*, 6334–6339.

Di Giambattista, M., Engelborghs, Y., Nyssen, E., & Cocito, C. (1987) *J. Biol. Chem. 262*, 8591–8597.

Grell, E., Oberbaumer, I., Ruf, H., & Zingsheim, H. P. (1977) *FEBS-Symp. No. 42*, 147–178.

Lakowicz, J. R., Laczko, G., & Gryczynski, I. (1986) *Rev. Sci. Instrum. 57*, 2499–2506.

Moureau, P., Engelborghs, Y., Di Giambattista, M., & Cocito, C. (1983) *J. Biol. Chem. 258*, 14233–14238.

Oberbaumer, I., Feigl, P., Ruf, H., & Grell, E. (1981) *Struct. Act. Nat. Pept., Proc. Fall Meet. Ges. Biol. Chem. 1979*, 523–538.

Schuster, P., Tortschanoff, K., & Winkler, H. (1976) *Z. Naturforsch. 31C*, 219–224.